Fine and hyperfine structures of pionic helium atoms

Zhi-Da Bai(白志达)[1,2], Zhen-Xiang Zhong(钟振祥)[1,†], Zong-Chao Yan(严宗朝)[3,1], and Ting-Yun Shi(史庭云)[1]

[1] *State Key Laboratory of Magnetic Resonance and Atomic and Molecular Physics, Wuhan Institute of Physics and Mathematics, Innovation Academy for Precision Measurement Science and Technology, Chinese Academy of Sciences, Wuhan* 430071, *China*

[2] *University of Chinese Academy of Sciences, Beijing* 100049, *China*

[3] *Department of Physics, University of New Brunswick, Fredericton, New Brunswick, E3B* 5A3, *Canada*

(Received 31 January 2022; revised manuscript received 14 April 2022; accepted manuscript online 7 May 2022)

The fine and hyperfine structures of pionic helium metastable states is calculated within the formalism of the Breit–Pauli Hamiltonian by using the variationally generated wave functions in Hylleraas coordinates. Our results not only verify the existing values of Hori *et al.* [*Phys. Rev. A* **89**, 042515 (2014)] for the fine structure of $\pi^4\mathrm{He}^+$, but also determine the hyperfine structure of $\pi^3\mathrm{He}^+$.

Keywords: exotic atom, pionic helium, fine structure, hyperfine structure

PACS: 36.10.–k, 31.15.aj, 31.15.ac **DOI:** 10.1088/1674-1056/ac6db9

1. Introduction

The pionic helium $\pi\mathrm{He}^+$ is a quasi-bound three-body atomic system consisting of a helium nucleus, an electron in the 1s orbital, and a π^- meson occupying a Rydberg state of large principal quantum number $n \sim 16$ and orbital angular momentum $\ell \sim n-1$. These states of $\pi\mathrm{He}^+$ are predicted to have a nanosecond-scale lifetime,[1] allowing for laser spectroscopy measurements. Recently, the transition $(n,\ell) = (17,16) \to (17,15)$ in $\pi^4\mathrm{He}^+$ was detected experimentally for the first time at Paul Scherrer Institute (PSI).[2] The next phase work of spectroscopy measurements at PSI is to push the measurement accuracy to the level of parts per billion (ppb),[3,4] so that a much improved value of π^- mass at ppb level could be derived in combination with high-precision quantum electrodynamic (QED) calculations. At this level of precision, knowledge about fine and hyperfine structures (for $\pi^3\mathrm{He}^+$) is essential for correctly determining the "central" spin-averaged transition frequency. So far, the study of the fine structure of $\pi^4\mathrm{He}^+$ and $\pi^3\mathrm{He}^+$ has been done in Ref. [1], but the hyperfine structure of $\pi^3\mathrm{He}^+$ has not yet been reported. The purpose of this paper is to conduct a comprehensive study of fine and hyperfine structures of some metastable states in $\pi^{3,4}\mathrm{He}^+$.

The structure of this paper is as follows. Section 2 describes the variational calculations of the wave functions under the closed-channel approximation.[5] Section 3 presents the theory of fine and hyperfine structures and numerical calculations of the associated coupling coefficients. Finally, a summary is given in Section 4. Atomic units ($e = \hbar = m_\mathrm{e} = 1$) are used throughout, unless otherwise stated. In order to facilitate a comparison with the previous calculations in Ref. [1], the same masses of π^- and ^{3,4}He nuclei are used, $m_\pi = 273.1320\,m_\mathrm{e}$,[6,7] $m_\mathrm{h} = 5495.8852754\,m_\mathrm{e}$, and $m_\alpha = 7294.2995361\,m_\mathrm{e}$,[7] without considering their uncertainties.

2. Variational wave functions

After removing the center of mass motion, the nonrelativistic Hamiltonian of a three-body Coulombic system can be written in the form of

$$H_0 = T + V, \tag{1}$$

where the kinetic and potential energy operators are, respectively,

$$T = \frac{1}{2\mu_1}\boldsymbol{p}_1^2 + \frac{1}{2\mu_2}\boldsymbol{p}_2^2 + \frac{1}{m_0}\boldsymbol{p}_1\cdot\boldsymbol{p}_2, \tag{2}$$

$$V = \frac{z_0 z_1}{r_1} + \frac{z_0 z_2}{r_2} + \frac{z_1 z_2}{r_{12}}. \tag{3}$$

Here the helium nucleus of mass m_0 is taken as the zeroth particle sitting at the origin of the reference frame, indices 1 and 2 are designated, respectively, for the electron and pion π^-, μ_1 and μ_2 are their reduced masses with respect to the helium nucleus, z_0, z_1, and z_2 are the charges of the three particles, and $\boldsymbol{r}_{12} = \boldsymbol{r}_1 - \boldsymbol{r}_2$.

Since any pion-excited states in $\pi\mathrm{He}^+$ are embedded in the singly excited electron continuum, these states are quasi-stable resonance states against Auger decay. Here we apply the Feshbach projection formalism[9,10] to seek the closed-channel quasi-bound solutions of H_0, using the variational principle.[11] The Rayleigh–Schrödinger variational principle can be extended to the excited states by Hylleraas–Undheim–McDonald theorem.[12] We introduce a pair of projection operators P and Q, which satisfy

$$P + Q = 1, \quad P^2 = P, \quad Q^2 = Q, \quad PQ = 0, \tag{4}$$

†Corresponding author. E-mail: zxzhong@wipm.ac.cn

© 2023 Chinese Physical Society and IOP Publishing Ltd

where P and Q are the usual open and closed channel operators, respectively. Only L^2-type wave functions are used to diagonalize the Hamiltonians QH_0Q and no open channel components are included.[13] The resonance eigenvalues deduced in above truncated diagonalization procedure would be upper bounds to the eigenvalues of QH_0Q.[13] In particular, the eigenvalue problem of QH_0Q,

$$(QH_0Q)Q\Psi = E_0Q\Psi \tag{5}$$

can be solved in the following variational Hylleraas basis:

$$\{r_1^\ell r_2^m r_{12}^n \mathrm{e}^{-\alpha r_1-\beta r_2-\gamma r_{12}}\mathcal{Y}^{LM}_{\ell_1\ell_2}(\hat{\boldsymbol{r}}_1,\hat{\boldsymbol{r}}_2)\}, \tag{6}$$

where α, β, and γ are real nonlinear parameters, and $\mathcal{Y}^{LM}_{\ell_1\ell_2}(\hat{\boldsymbol{r}}_1,\hat{\boldsymbol{r}}_2)$ is the (ℓ_1,ℓ_2)-coupled spherical harmonics to form a common eigenstate of $\boldsymbol{L}^2$ and L_z. The nonlinear parameters are optimized by minimizing the energy eigenvalues, which involves computing the energy gradients in the parameter space.[15,16] The variational eigenvalues of the excited states are also upper bounds to the respective exact energies according to Hylleraas–Undheim–McDonald theorem.[12] If a basis function is added, the original $\mathcal{N}\times\mathcal{N}$ becomes an $(\mathcal{N}+1)\times(\mathcal{N}+1)$ matrix. Then the old excited-state eigenvalues interleave the new eigenvalues and can never "fall through" the exact energies. In our work, the eigenvector $Q\Psi$ is expanded by a basis set which is divided into several blocks with ℓ_1 satisfying $\ell_1 < \Delta\ell$, where $\Delta\ell = \ell - \ell'$ is the multipolarity, i.e., the smallest energetically possible change of the pionic orbital angular momentum in the Auger decay,[17] and each ℓ_1-block has its own set of nonlinear parameters. In order to enhance the rate of convergence, we further divide the leading configuration $(\ell_1,\ell_2) = (0,L)$ into 4 subgroups each having its own nonlinear parameters. The basis set is generated by including all terms such that $\ell+m+n \le \Omega$, where the integer Ω controls the size of basis set. More details about the construction of a basis set can be found in Ref. [18]. Given the uncertainty for PSI planned experiments targeting an MHz level, our closed-channel solutions for fine and hyperfine structures in $\pi\mathrm{He}^+$ should suffice. Of course, we can always switch to full calculation using the theory of complex coordinate rotation (CCR) if necessary. Table 1 contains a convergence study of the nonrelativistic energy for the state (17,16) of $\pi^4\mathrm{He}^+$, as the size of basis set $\mathcal{N}$ enlarges progressively, where the ratio R is defined by

$$R(\Omega) = \frac{E_0(\Omega-1)-E_0(\Omega-2)}{E_0(\Omega)-E_0(\Omega-1)}, \tag{7}$$

and the extrapolated energy is determined by[19]

$$E_0(\infty) = E_0(\Omega) + \frac{E_0(\Omega)-E_0(\Omega-1)}{R-1}. \tag{8}$$

The uncertainty is taken to be the difference between $E_0(\infty)$ and $E_0(\Omega_{\mathrm{Max}})$. Our calculated energy agrees with the value of Hori *et al.*[1] The convergence study for the other energy levels is similar to the (17,16) state. It should be noted that the precision of closed-channel approximation within Feshbach formalism is limited by the width of the metastable states.[11] Thus, for some short-lived state such as (15,14), the present results have less converged digits. The accuracy of expectation values of other operators is limited by the precision of nonrelativistic wave functions.

Table 1. Convergence study of the energy eigenvalue and some reduced matrix elements for the state $(17,16)$ of $\pi^4\mathrm{He}^+$.

Ω	$\mathcal{N}$	E_0	R	T_1	T_2	$S_2^{(1)}$	$S_2^{(2)}$
10	580	−2.65751243837334		−0.32722364	21.77670515305	−55.91192037	358.4220732531
11	780	−2.65751243846377		−0.32722740	21.77670527013	−55.91189769	358.4220750972
12	1025	−2.65751243849889	2.57	−0.32725275	21.77670528884	−55.91188926	358.4220753943
13	1320	−2.65751243850054	21.3	−0.32724727	21.77670529192	−55.91188431	358.4220754457
14	1670	−2.65751243850125	2.32	−0.32724606	21.77670529242	−55.91188131	358.4220754539
15	2080	−2.65751243850162	1.92	−0.32724761	21.77670529328	−55.91188003	358.4220754650
Extrap.		−2.657512438502(1)		−0.327247(1)	21.776705291(3)	−55.911879(5)	358.42207542(5)
Hori *et al.*[1]		−2.65751243850171					

3. Fine and hyperfine structures

The spin dependent part of the Breit–Pauli Hamiltonian[20,21] is responsible for the leading-order fine and hyperfine structures. For a pionic helium where the spin of pion is zero, the spin–orbital interaction is

$$\begin{aligned} V_{\mathrm{so}} = \alpha^2\Bigg[&\frac{z_0z_1}{2m_0^2}(1+2a_0)\frac{\boldsymbol{r}_1}{r_1^3}\times\boldsymbol{p}_0\cdot\boldsymbol{s}_0 - \frac{z_1g_0}{2m_0m_1}\frac{\boldsymbol{r}_1}{r_1^3}\times\boldsymbol{p}_1\cdot\boldsymbol{s}_0 \\ &-\frac{z_0z_1}{2m_1^2}(1+2a_1)\frac{\boldsymbol{r}_1}{r_1^3}\times\boldsymbol{p}_1\cdot\boldsymbol{s}_1 + \frac{z_0g_1}{2m_0m_1}\frac{\boldsymbol{r}_1}{r_1^3}\times\boldsymbol{p}_0\cdot\boldsymbol{s}_1 \\ &+\frac{z_0z_2}{2m_0^2}(1+2a_0)\frac{\boldsymbol{r}_2}{r_2^3}\times\boldsymbol{p}_0\cdot\boldsymbol{s}_0 - \frac{z_2g_0}{2m_0m_2}\frac{\boldsymbol{r}_2}{r_2^3}\times\boldsymbol{p}_2\cdot\boldsymbol{s}_0 \\ &-\frac{z_1z_2}{2m_1^2}(1+2a_1)\frac{\boldsymbol{r}_{12}}{r_{12}^3}\times\boldsymbol{p}_1\cdot\boldsymbol{s}_1 + \frac{z_2g_1}{2m_1m_2}\frac{\boldsymbol{r}_{12}}{r_{12}^3}\times\boldsymbol{p}_2\cdot\boldsymbol{s}_1\Bigg], \end{aligned} \tag{9}$$

and the spin–spin one is

$$\begin{aligned} V_{\mathrm{ss}} = \alpha^2\frac{g_0g_1}{4m_0m_1}\Bigg[&\frac{\boldsymbol{s}_0\cdot\boldsymbol{s}_1}{r_1^3} - \frac{3(\boldsymbol{r}_1\cdot\boldsymbol{s}_0)(\boldsymbol{r}_1\cdot\boldsymbol{s}_1)}{r_1^5} \\ &-\frac{8\pi}{3}\delta(\boldsymbol{r}_1)(\boldsymbol{s}_0\cdot\boldsymbol{s}_1)\Bigg], \end{aligned} \tag{10}$$

where $\boldsymbol{p}_0 = -\boldsymbol{p}_1 - \boldsymbol{p}_2$, $\boldsymbol{s}_0$ is the helion spin, and $\boldsymbol{s}_1$ is the electron spin. In the above, $g_0 = g_{\rm h}(m_{\rm h}/m_{\rm p}) = -12.736614736(50)$ and $a_0 = g_0/4 - 1 = -4.184153684(12)$, with $g_{\rm h}$ being the helion's g-factor, $m_{\rm h}/m_{\rm p}$ the heloin–proton mass ratio, and a_0 the helion's magnetic moment anomaly.[7] Similarly, the electron g-factor is $g_1 = g_{\rm e} = -2.00231930436153(53)$ and the magnetic moment anomaly is $a_1 = a_{\rm e} = 1.15965218076(27) \times 10^{-3}$.[7] The corrections due to the finite nuclear size effect is negligible at the current accuracy.[8]

Table 2. Expectation values of various operators for $\pi^4{\rm He}^+$.

(n,L)	T_1	T_2	T_{12}	$S_1^{(1)}$	$S_1^{(2)}$	$S_1^{(12)}$
(15,14)	−0.299(2)	59.46(1)	3.2212(2)	0.1316(2)	−2.21(1)	−0.2906(2)
(16,15)	−0.3239(2)	36.34955(2)	3.43468(1)	0.096856(3)	−1.09904(3)	−0.22422(2)
(17,15)	−0.296(3)	26.516(5)	3.0939(3)	0.0691(2)	−0.89(2)	−0.159(2)
(18,15)	−0.25(2)	19.8(2)	2.606(2)	0.051(1)	−0.7(1)	−0.116(1)
(17,16)	−0.327247(1)	21.776705291(3)	3.43967(1)	0.0681181(3)	−0.54448859(2)	−0.1641717(1)
(18,16)	−0.28045(3)	15.87762(1)	2.868296(3)	0.047022(3)	−0.42295(3)	−0.112684(3)
(19,16)	−0.232(3)	12.01(2)	2.307(2)	0.03422(3)	−0.341(3)	−0.0811(1)
(18,17)	−0.30892(2)	12.6931646(3)	3.18904(1)	0.04404031(2)	−0.25818877(2)	−0.1100914(3)
(19,17)	−0.2513(2)	9.498(1)	2.5108(2)	0.0311777(3)	−0.205449(1)	−0.07702(5)
(19,18)	−0.27132(5)	7.2919(2)	2.71760(2)	0.026126(2)	−0.117635(3)	−0.06733(2)
(n,L)	$S_2^{(1)}$	$S_2^{(2)}$	$S_2^{(12)}$	$\delta(\boldsymbol{r}_1)$	$\delta(\boldsymbol{r}_{12})$	
(15,14)	−65.89(2)	858.5(2)	127.66(2)	1.2714457(1)	0.0807435(1)	
(16,15)	−62.22474(3)	561.63353(3)	122.47557(5)	1.49518439(1)	0.060627193(1)	
(17,15)	−48.66(3)	409.5(3)	95.685(3)	1.762600(3)	0.0402463(3)	
(18,15)	−37.3(1)	305(1)	73.3(2)	1.96693(4)	0.026982(3)	
(17,16)	−55.911879(5)	358.42207542(5)	110.89895(2)	1.7300409888(3)	0.04112256448(3)	
(18,16)	−42.1029(1)	261.2913(1)	83.47261(1)	1.960760468(1)	0.0267217115(3)	
(19,16)	−31.92(1)	197.5(1)	63.25(3)	2.119201966(3)	0.0184277380(1)	
(18,17)	−47.0029(1)	221.68267(2)	93.599562(1)	1.959448215(5)	0.02455291(3)	
(19,17)	−34.914(3)	165.86(2)	69.494(5)	2.128520(3)	0.01644984(5)	
(19,18)	−36.897(3)	134.674(3)	73.626(2)	2.1566765(2)	0.0127411495(5)	

Table 3. Expectation values of various operators for $\pi^3{\rm He}^+$.

(n,L)	T_1	T_2	T_{12}	$S_1^{(1)}$	$S_1^{(2)}$	$S_1^{(12)}$
(15,14)	−0.301(5)	56.86(3)	3.2358(5)	−65.12(5)	820.9(5)	126.28(3)
(16,15)	−0.3235(3)	34.60724(2)	3.4337(2)	−61.2233(2)	534.71873(5)	120.5502(2)
(18,15)	−0.251(3)	18.8(1)	2.567(1)	−36.38(3)	290.1(3)	71.49(3)
(17,16)	−0.32499(1)	20.61585741(1)	3.415283(3)	−54.64404(1)	339.3178092(3)	108.403397(3)
(18,16)	−0.277(2)	15.026(2)	2.8246(1)	−40.96954(3)	247.27(2)	81.239(2)
(19,16)	−0.2274(3)	11.381(3)	2.2611(5)	−31.02(1)	187.3(2)	61.47(2)
(18,17)	−0.304567(3)	11.9486744(5)	3.137865(2)	−45.55247(3)	208.68133(2)	90.717796(3)
(19,17)	−0.2464(1)	8.966(2)	2.4573(2)	−33.802(5)	156.58(2)	67.28(2)
(19,18)	−0.26536(3)	6.8444(2)	2.64855(2)	−35.479(2)	126.411(3)	70.798(2)
(n,L)	$S_2^{(1)}$	$S_2^{(2)}$	$S_2^{(12)}$	$\delta(\boldsymbol{r}_1)$	$\delta(\boldsymbol{r}_{12})$	
(15,14)	0.1318(5)	−2.12(3)	−0.2914(3)	1.289855(2)	0.0789368(2)	
(16,15)	0.09709(2)	−1.06053(3)	−0.224553(5)	1.51646197(2)	0.058703890(2)	
(18,15)	0.0509(3)	−0.69(2)	−0.115(2)	1.9847517(5)	0.0259699(2)	
(17,16)	0.0681209(1)	−0.52418984(3)	−0.1636996(1)	1.75315960494(5)	0.039295608673(2)	
(18,16)	0.04709(3)	−0.4061(2)	−0.11242(1)	1.97967151(3)	0.025479541(2)	
(19,16)	0.034366(3)	−0.3269(2)	−0.08112(5)	2.133248035(3)	0.017621752(3)	
(18,17)	0.04396249(3)	−0.24819456(3)	−0.1092366(2)	1.981842(2)	0.0230670(1)	
(19,17)	0.031318(2)	−0.1980153(2)	−0.07684(3)	2.144415(2)	0.0155362(2)	
(19,18)	0.026184(1)	−0.113723(2)	−0.066744(5)	2.175099(1)	0.011759334(1)	

Since the ^{4}He nucleus also has zero spin, the effective Hamiltonian of the fine-structure of $\pi^4\mathrm{He}^+$ is

$$H_{\mathrm{eff}} = \varepsilon_1(\boldsymbol{L}\cdot\boldsymbol{s}_1), \tag{11}$$

where the fine-structure coefficient ε_1 can be calculated by integrating Eq. (9) over spatial degrees of freedom. On the other hand, the effective Hamiltonian of the fine and hyperfine structures of $\pi^3\mathrm{He}^+$ is

$$\begin{aligned} H_{\mathrm{eff}} =\ & \varepsilon_1(\boldsymbol{L}\cdot\boldsymbol{s}_1)+\varepsilon_2(\boldsymbol{L}\cdot\boldsymbol{s}_0)+\varepsilon_3(\boldsymbol{s}_0\cdot\boldsymbol{s}_1) \\ & +\varepsilon_4\{2L(L+1)(\boldsymbol{s}_0\cdot\boldsymbol{s}_1)-3[(\boldsymbol{L}\cdot\boldsymbol{s}_0)(\boldsymbol{L}\cdot\boldsymbol{s}_1) \\ & +(\boldsymbol{L}\cdot\boldsymbol{s}_1)(\boldsymbol{L}\cdot\boldsymbol{s}_0)]\}, \end{aligned} \tag{12}$$

where the corresponding fine- and hyperfine-structure coefficients are ε_1, ε_2, ε_3, and ε_4. The relevant reduced matrix elements involved in calculating ε_i are

$$\begin{aligned} S_j^{(i)} &= \left\langle \left\| \frac{1}{r_i^3}(\mathrm{i}\boldsymbol{r}_i\times\nabla_{\boldsymbol{r}_j}) \right\| \right\rangle, \\ S_j^{(12)} &= \left\langle \left\| \frac{1}{r_{12}^3}(\mathrm{i}\boldsymbol{r}_{12}\times\nabla_{\boldsymbol{r}_j}) \right\| \right\rangle, \\ T_i &= \left\langle \left\| \frac{1}{r_i^5}[\boldsymbol{r}_i\otimes\boldsymbol{r}_i]^{(2)} \right\| \right\rangle, \\ T_{12} &= \left\langle \left\| \frac{1}{r_{12}^5}[\boldsymbol{r}_{12}\otimes\boldsymbol{r}_{12}]^{(2)} \right\| \right\rangle, \end{aligned} \tag{13}$$

where $i,j=1,2$. A convergence study of T_1, T_2, $S_2^{(1)}$, and $S_2^{(2)}$ for $(17,16)$ of $\pi^4\mathrm{He}^+$ is presented in Table 1. The numerical values of all the reduced matrix elements defined in Eq. (13), together with $\delta(r_1)$ and $\delta(r_{12})$, are listed in Tables 2 and 3 for $\pi^4\mathrm{He}^+$ and $\pi^3\mathrm{He}^+$, respectively. The coupling of the electron spin $\boldsymbol{s}_1$ with the π^- orbital angular momentum $\boldsymbol{L}$ splits a $\pi^4\mathrm{He}^+$ state (n,L) into two substates of the total angular momentum $\boldsymbol{J}=\boldsymbol{L}+\boldsymbol{s}_1$: $L+1/2$ and $L-1/2$. Table 4 presents the nonrelativistic energies E_0, the fine structure coefficients ε_1, and the fine-structure state energies relative to E_0 for various $\pi^4\mathrm{He}^+$ states. The uncertainties of these fine structure energies include the computational errors and the errors due to the uncalculated QED corrections of order $m\alpha^6$. For those shorter-lived states, the former dominates the latter. For $\pi^3\mathrm{He}^+$, one needs to further couple $\boldsymbol{J}=\boldsymbol{L}+\boldsymbol{s}_1$ with the helion spin $\boldsymbol{s}_0$ to form the total angular momentum $\boldsymbol{F}=\boldsymbol{J}+\boldsymbol{s}_0$. Numerical results are shown in Tables 5 and 6 for the fine-structure coefficients and hyperfine structure energy levels of $\pi^3\mathrm{He}^+$, respectively. Our results for ε_1 are in good agreement with the values of Hori *et al.*[1] It can be seen that the fine-structure splittings are around several tens of GHz, and the hyperfine splittings are around several GHz, which can be detected in future PSI experiments. The uncertainty of the fine-structure splittings in (17,16) and (16,15) of $\pi^4\mathrm{He}^+$ is about 1 MHz.

Table 4. Nonrelativistic energies E_0, fine-structure coefficients ε_1, and fine-structure state energies relative to E_0, designated by the total angular momentum $J=L\pm1/2$, for the case of $\pi^4\mathrm{He}^+$. The second entries are from Ref. [1] for comparison.

(n,L)	E_0 (a.u.)	ε_1 (MHz)	$L+1/2$ (GHz)	$L-1/2$ (GHz)
(16,15)	−2.828549393(1)	−1955.0(1)	−14.6625(8)	15.6400(8)
	−2.82854939373(4)	−1954.99		
(15,14)	−3.0569(1)	−2243.6(10)	−15.705(8)	16.827(8)
	−3.0569481417(4)	−2244.04		
(17,16)	−2.657512438502(1)	−1611.79(9)	−12.8943(8)	13.7002(8)
	−2.65751243850171	−1611.79		
(17,15)	−2.68543(1)	−1521(4)	−11.41(3)	12.17(3)
	−2.68542722(2)	−1521.19		
(18,15)	−2.58002(1)	−1161(5)	−8.71(4)	9.29(4)
	−2.58002554(1)	−1159.48		
(18,16)	−2.55698492(1)	−1208.78(6)	−9.6702(5)	10.2746(5)
	−2.556984919572(2)	−1208.78		
(18,17)	−2.531946569(1)	−1242.56(7)	−10.5618(6)	11.1830(7)
	−2.5319465695913(1)	−1242.56		
(19,16)	−2.48154(1)	−913.2(5)	−7.306(4)	7.762(5)
	−2.48154055239(1)	−913.16		
(19,17)	−2.461806(1)	−919.7(1)	−7.8175(9)	8.2773(9)
	−2.4618067856861(1)	−919.72		
(19,18)	−2.4413857(1)	−895.65(5)	−8.0609(5)	8.5087(5)
	−2.4413857971745(1)	−895.64		

Table 5. Nonrelativistic energies E_0 and fine and hyperfine-structure coefficients ε_i, $i = 1,2,3,4$, for the case of $\pi^3\mathrm{He}^+$. The second entries are from Ref. [1] for comparison.

(n,L)	E_0 (a.u.)	ε_1 (MHz)	ε_2 (MHz)	ε_3 (MHz)	ε_4 (MHz)
(16,15)	−2.81027798(1)	−1947.2(1)	−10.1401(5)	−5163.9(3)	0.02464(2)
	−2.810277989054(3)	−1947.18			
(15,14)	−3.03425(1)	−2247(2)	−17.15(1)	−4392.2(2)	0.0271(5)
	−3.0342533945(3)	−2247.04			
(17,16)	−2.6431226103(1)	−1593.92(8)	−5.8720(3)	−5969.9(3)	0.021165(1)
	−2.64312261030188(2)	−1593.92			
(18,15)	−2.56848(3)	−1145(4)	−5.490(6)	−6758.5(4)	0.0191(2)
	−2.568490191(5)	−1145.39			
(18,16)	−2.54564547(1)	−1190.2(1)	−4.2671(4)	−6741.2(4)	0.0180(1)
	−2.545645472099(1)	−1190.19			
(18,17)	−2.520881426(1)	−1218.10(6)	−3.3044(2)	−6748.6(4)	0.0171169(9)
	−2.52088142679	−1218.10			
(19,16)	−2.47237(1)	−897.9(3)	−3.227(3)	−7264.2(4)	0.01481(2)
	−2.47237023589(1)	−897.91			
(19,17)	−2.452936(1)	−900.7(3)	−2.4731(3)	−7302.2(4)	0.013847(6)
	−2.4529359745011	−900.79			
(19,18)	−2.4329808(1)	−870.97(5)	−1.8339(1)	−7406.7(4)	0.012976(1)
	−2.4329808449305	−870.97			

Table 6. Hyperfine structure state energies (in units of GHz), relative to the nonrelativistic energies, for the case of $\pi^3\mathrm{He}^+$, where the hyperfine states are designated by (J,F).

(n,L)	$(L+1/2,L+1)$	$(L+1/2,L)$	$(L-1/2,L)$	$(L-1/2,L-1)$
(16,15)	−15.9764(8)	−13.3643(8)	16.9367(8)	14.3612(8)
(15,14)	−16.95(2)	−14.57(2)	17.91(2)	15.88(2)
(17,16)	−14.2961(7)	−11.4501(7)	15.2464(7)	12.0995(7)
(18,15)	−10.32(3)	−7.37(3)	11.33(3)	7.51(3)
(18,16)	−11.2455(8)	−8.2617(8)	12.2393(8)	8.4623(8)
(18,17)	−12.0739(6)	−9.0613(6)	13.0567(6)	9.2998(6)
(19,16)	−9.029(3)	−6.081(3)	10.171(3)	5.839(3)
(19,17)	−9.506(3)	−6.514(3)	10.625(3)	6.298(3)
(19,18)	−9.7110(5)	−6.6844(5)	10.8330(5)	6.4352(5)

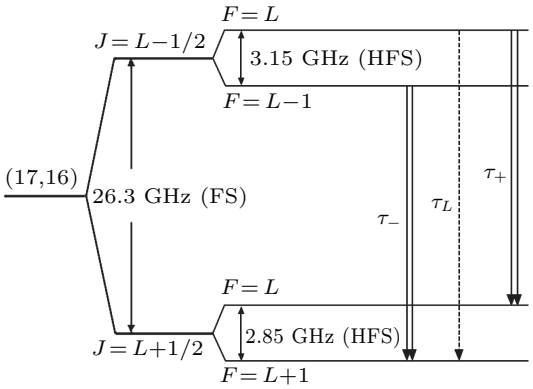


Fig. 1. Schematic diagram of hyperfine sublevels of the (17,16) state of $\pi^3\mathrm{He}^+$ atom.

Figure 1 shows three transitions within the (17, 16) manifold of $\pi^3\mathrm{He}^+$. Using the values listed in Table 6, one can obtain the theoretical values for the transition frequencies

$$\begin{aligned} \tau_+ &= 26696.5(10)\ \text{MHz}, \\ \tau_- &= 26395.6(10)\ \text{MHz}. \end{aligned} \tag{14}$$

The difference between τ_+ and τ_- is nearly proportional to the helion magnetic moment[22] and has a value

$$\Delta\tau = 300.9(14)\ \text{MHz}. \tag{15}$$

It is noted that measurements of hyperfine structure in antiprotonic helium $\bar{\mathrm{p}}^4\mathrm{He}^+$ have been performed by the ASACUSA group,[23,24] which agree with QED calculations[22] of order $m\alpha^6$. Thus, our theoretical prediction in Eq. (14) for $\pi^3\mathrm{He}^+$ may provide a reference for future experiments at PSI. However, in order to achieve improved theoretical results for τ_+ and τ_-, a complete QED calculation of order $m\alpha^6$ is required to provide corrections to the coefficients ε_1–ε_4.

4. Summary

In conclusion, the wave functions along with the corresponding nonrelativistic energies were calculated variationally by using Hylleraas-type basis sets within the Feshbach closed-channel approximation. For long-lived states, energy eigenvalues were calculated to a precision of 10^{-10}. But for short-lived states, the numerical uncertainties were quite large due to large widths. In this case, the CCR method can be used to improve the numerical accuracy.[25,26] The expectation values of the Breit operators were evaluated perturbatively. We presented the results of the fine and hyperfine structures for some experimentally relevant metastable states of $\pi^{3,4}\mathrm{He}^+$ within the framework of the Breit–Pauli Hamiltonian, at 10^{-4} level of accuracy. In particular, the hyperfine-structure coefficients of $\pi^3\mathrm{He}^+$ were calculated for the first time. Our work will provide useful information for future precision measurements on pionic helium systems.

Acknowledgements

Project supported by the National Natural Science Foundation of China (Grant Nos. 11974382 and 11474316). ZCY acknowledges the support from NSERC and SHARCnet of Canada.

References

[1] Hori M, Sótér A and Korobov V I 2014 *Phys. Rev. A* **89** 042515
[2] Hori M, Aghai-Khozani H, Sótér A, Dax A and Barna D 2020 *Nature* **581** 37
[3] Hori M, Aghai-Khozani H, Sótér A, Dax A and Barna D 2021 *Few-Body Syst.* **62** 1
[4] Hori M, Aghai-Khozani H, Sótér A, Dax A and Barna D 2021 *SciPost Phys. Proc.* **5** 26
[5] Korobov V I, Bakalov D and Monkhorst H J 1999 *Phys. Rev. A* **59** R919
[6] Beringer J, Arguin J F, Barnett R M, *et al.* 2012 *Phys. Rev. D* **86** 010001
[7] Mohr P J, Taylor B N and Newell D B 2012 *Rev. Mod. Phys.* **84** 1527
[8] Eides M I, Grotch H and Shelyut V A 2001 *Phys. Rep.* **342** 63
[9] Feshbach H 1962 *Ann. Phys.* **19** 287
[10] Hahn Y, O'Malley T F and Spruch L 1962 *Phys. Rev. A* **128** 932
[11] Hu M, Yao S, Wang Y, Li W, Gu Y and Zhong Z 2016 *Chem. Phys. Lett.* **654** 114
[12] Drake G W F 2020 *J. Phys. B* **53** 223001
[13] Altick P L and Moore E N 1965 *Phys. Rev. Lett.* **15** 100
[14] Perkins J F 1969 *Phys. Rev.* **178** 89
[15] Cassar M M and Drake G W F 2004 *J. Phys. B* **37** 2485
[16] Zhong Z, Tong X, Yan Z and Shi T 2015 *Chin. Phys. B* **24** 053102
[17] Korobov V I 2003 *Phys. Rev. A* **67** 062501
[18] Yan Z, Zhang J and Li Y 2003 *Phys. Rev. A* **67** 062504
[19] Drake G W F and Yan Z 1994 *Chem. Phys. Lett.* **229** 486
[20] Bethe H A and Salpeter E E 2012 *Quantum mechanics of one-and two-electron atoms* (Springer Science & Business Media)
[21] Berestetskii V B, Lifshitz E M and Pitaevskii L P 1982 *Quantum Electrodynamics* (Butterworth-Heinemann)
[22] Korobov V I and Zhong Z X 2009 *Phys. Rev. A* **80** 042506
[23] Pask T, Barna D, Dax A, Hayano R S, Hori M, Horváth D, Juhász B, Malbrunot C, Marton J, Ono N, Suzuki K, Zmeskal J and Widmann E 2008 *J. Phys. B* **41** 081008
[24] Pask T, Barna D, Dax A, Hayano R S, Hori M, Horváth, Friedreich S, Juhász B, Massiczek O, Ono N, Sótér A and Widmann E 2009 *Phys. Lett. B* **678** 55
[25] Ho Y K 1983 *Phys. Rep.* **99** 1
[26] Bai Z D, Zhong Z X, Yan Z C and Shi T Y 2021 *Chin. Phys. B* **30** 023101